International Journal on
"Technical and Physical Problems of Engineering"
(IJTPE)
Published by International Organization of IOTPE

ISSN 2077-3528
IJTPE Journal
www.iotpe.com
ijtpe@iotpe.com

December 2022 | Issue 53 | Volume 14 | Number 4 | Pages 392-399

A ROBUST METAHEURISTIC CENTRAL CONTROLLER FOR HIERARCHICAL CONTROL SYSTEM WITH ADAPTIVE POWER SHARING AND MPPT IN DC MICROGRIDS

E. Yusubov L.R. Bekirova

Instrumentation Engineering Department, Azerbaijan State Oil and Industry University, Baku, Azerbaijan
elvinyusifov05@gmail.com, lala_bekirova@mail.ru

Abstract- This article presents a robust metaheuristic central controller for the hierarchical control system with adaptive power sharing and MPPT in DC microgrids using the metaheuristic moth-flame optimization (MFO) algorithm to extract maximum power and improve power sharing in DC microgrids. Maximum power extraction from the photovoltaic modules and equal distribution of this power among the units are the primary factors causing the power loss and increased stresses in DC microgrids. Maximum power point tracking (MPPT) and primary controllers are employed to ensure maximum power extraction and power sharing, respectively. Although conventional MPPT controllers, perform well under uniform solar irradiation, they underperform when PV modules are partially shaded. Furthermore, traditional droop-based primary controllers are relatively simpler and more effective under normal conditions. However, their adaptivity to dynamic variations is not satisfactory. In this article, a unified control strategy is proposed to overcome the above-mentioned shortcomings of both controllers by using an MFO-based central controller. The proposed central controller also merges the functions of the tertiary, which is adopted to control total power flow among the DC microgrids or DC microgrids and the utility grid, and the secondary controller, which is necessary for the reduction of DC link voltage deviations. Simulation results verify the proposed control technique's efficiency.

Keywords: Power Electronics, DC Microgrid, Droop Control, MPPT Control, DC-DC Converters.

1. INTRODUCTION

The popularity of DC microgrids (DCMG) is rapidly growing owing to their integration capabilities of various distributed energy resources (DER) [1]. PV, fuel cells, and battery packs are prime examples of DERs. Most of the issues present in the AC microgrids such as reactive power, frequency synchronization, and AC/DC conversions do not exist in DCMGs, which are the advantages of DCMGs [2]. Figure 1 presents simplified block diagram of DCMGS with PV inputs. Being one of key components of DCMGs, DC-DC converters output stable voltage under input PV voltage variations.

The non-linear power-output (*P-V*) characteristics of PV modules require the usage of MPPT controllers for the extraction of maximum power. Partial shading is a phenomenon in which a certain section of the PV modules is covered. Shaded cells can act as a load and instead of generating power, they can consume the power resulting in power loss. Bypass diodes are used to prevent shaded cells to consume the power [3]. However, it generates multiple peaks in the *P-V* characteristics of the modules. Under partial shading, existing MPPT control algorithms include the popular Perturb and Observe [4-6], Incremental conductance [7-10] as well as intelligent fuzzy [11-13], and metaheuristic PSO-based methods [14-17]. Traditional methods for MPPT may detect only one peak, which could be the local maxima, instead of the global maxima. The fuzzy controllers produce better results under partial shading, but the design process can be time-consuming and their overall operational efficiency depends on human expertise. The literature on metaheuristic PSO-MPPT controllers is vast. Although these controllers can detect the global peak, their convergence time is not satisfactory.

In DCMGs, output voltages of parallel units are not equal, which causes circulating issues among the converters. Unless it is properly handled, the stress that is put on some of the converters can be overwhelming, thereby decreasing the reliability of the DCMG. Primary controllers are responsible for ensuring the proper power/current sharing among units [18]. One of the popular and easily implemented methods for power sharing is the droop control method [19-21]. However, traditional droop controllers are not adaptive to the variations. A hierarchical control system utilizes primary, secondary, and tertiary controllers to implement the control of a whole DCMG [22]. This article aims at building a hierarchical control system that proposes a unified metaheuristic strategy for controlling both MPPT and current sharing for maximum efficiency. The proposed strategy involves two DC-DC converters between the PV unit and DC common link. The first converter, which is directly connected to the PV module, is controlled by the MPPT controller to output maximum power.

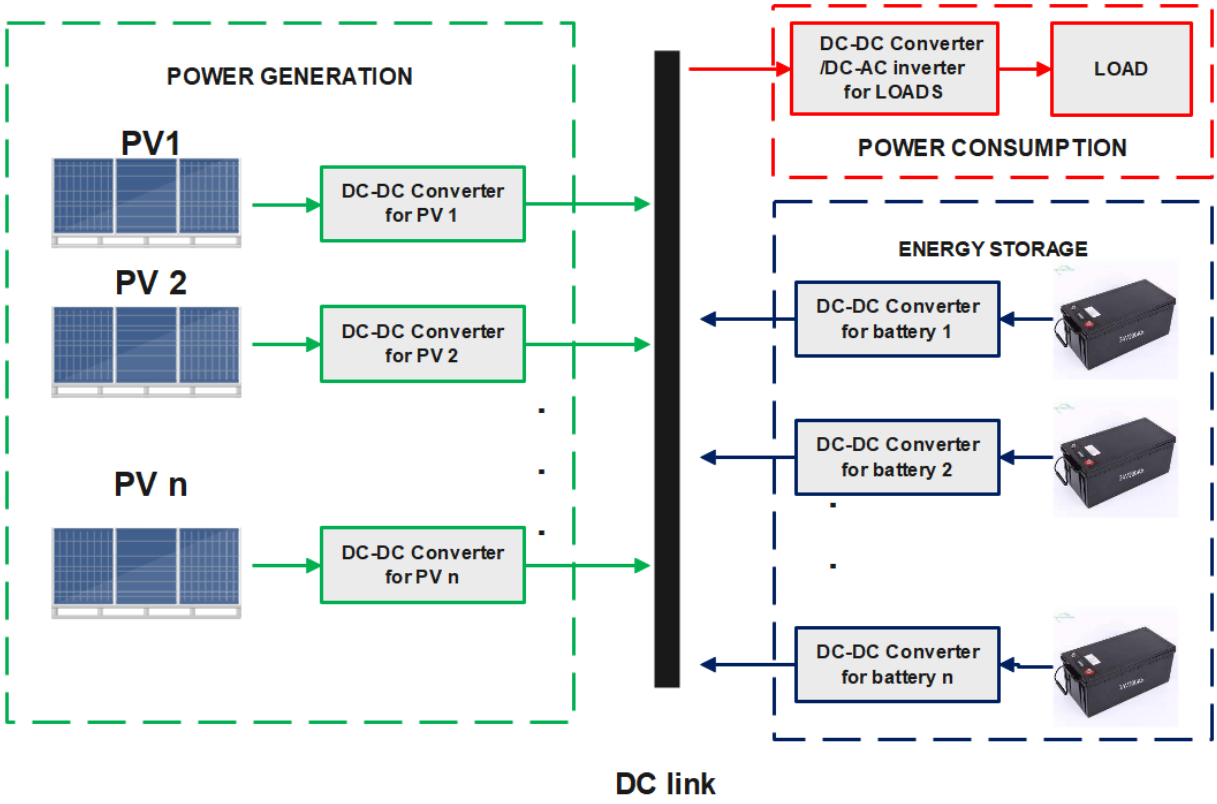

Figure 1. Simple PV input DC microgrid [22]

The second DC-DC converter inputs the maximum delivered power from the first converter to regulate DC link voltage and it is controlled by a hierarchical strategy.

2. MOTH-FLAME OPTIMIZATION (MFO)

The algorithm initiates the randomly generated moths' positions by the P matrix (1) representing the potential solutions [23].

$$P=\begin{pmatrix} p_{11} & p_{12} & \cdots & p_{1d} \\ p_{21} & p_{22} & \cdots & p_{2d} \\ \cdots & \cdots & \cdots & \cdots \\ p_{n1} & p_{n2} & \cdots & p_{nd} \end{pmatrix} \quad (1)$$

where, n and d stand for the total of moths and dimension, respectively.

The following formula (2) with a random moth generator is utilized for the moth positions [23].

$$P_{ij}=\left(UL(i)-LL(i)\right)\text{rand}()+LL(i) \quad (2)$$

where, UL and LL define upper and lower limits, respectively. The generation of the fitness function array (3) is necessary for every moth [23].

$$OP=\begin{pmatrix} OP_1 \\ OP_2 \\ \vdots \\ OP_n \end{pmatrix} \quad (3)$$

Another significant element of the algorithm is the flames representing the best potential solutions at the time. The flame and its fitness function matrices can be expressed in (4) and (5), respectively [23].

$$F=\begin{pmatrix} F_{11} & F_{12} & \cdots & F_{1d} \\ F_{21} & F_{22} & \cdots & F_{2d} \\ \cdots & \cdots & \cdots & \cdots \\ F_{n1} & F_{n2} & \cdots & F_{nd} \end{pmatrix} \quad (4)$$

$$OF=\begin{pmatrix} OF_1 \\ OF_2 \\ \vdots \\ OF_n \end{pmatrix} \quad (5)$$

The logarithmic spiral function is selected as moth position updater (6) [24].

$$S\left(P_i,F_j\right)=D_i e^{bt}\cos(2\pi t)+F_j \quad (6)$$

$$D_i=\left|F_j-P_j\right| \quad (7)$$

where, D is the distance between the moth and the relevant flame. For better exploitation, the number of flames reduces (8) [23].

$$FlameNumber=\text{round}(N-L\times\frac{N-L}{T}) \quad (8)$$

where, N, l, and T stand for the total number of flames, and the actual and total iteration numbers.

The algorithm also has superior exploration capability, which prevents the local optima problem and help determine the global peak. However, the exploitation capability is also necessary to ensure the balance with the exploration. In the proposed algorithm, the number of moths is defined to be 25, while that of iterations are 70.

Algorithm 1. The MFO pseudo-code [23]

```
random moth position initialization
for i=1to n do
    the evaluation function computation
while iteration ≤ Max iteration do
    update P_i
    Compute the flame number
    Compute evaluation function f_i
    if iteration==1 then
        F=sort ( P ) and OF=sort ( OP )
    else
        F=sort ( P_{t-1}, P_t ) and OF=sort ( OP_{t-1}, OP_t )
    end if
    for i = to n do
        for i =1 to d do
        Compute D value
        P(i, j) update
        end for
end while
```

3. DC MICROGRID CONTROL

3.1. MPPT Control

MPPT controllers are used in the proposed DCMG to increase efficiency. Figures 2 and 3 display the simple and proposed PV-DC microgrid with the MPPT control strategy, respectively.

3.1.1. Perturb and Observe

Perturb and Observe (PO is one of the prominent examples of the conventional MPPT control, which can be performed with two methods. In the first method, the reference voltage of the converter is the output, while the second method utilizes the direct duty cycle method. The PO starts by taking the current and voltage measurements of the PV unit, after which the changes in power and voltage have been observed. The result of these changes determines the ratio of the duty cycle to the converter, which is given in Table 1 [5].

Table 1. Change of Duty ration in PO method [5]

Perturb and observe	$\Delta P>0$	$\Delta P<0$
$\Delta V>0$	$D+\Delta D$	$D-\Delta D$
$\Delta V<0$	$D-\Delta D$	$D+\Delta D$

The main advantages of the PO method are its simplicity and easy implementation. It is also effective under uniform solar irradiation. However, it may not detect the global peak, under partial shading.

3.1.2. Particle Swarm Optimization

Being one of the most utilized metaheuristic algorithms in engineering and theoretical studies, PSO was inspired by the unified bird/fish group behavior and can be represented as Equations (9) and (10) [15].

$$z_i^{t+1} = z_i^t + v_i^{t+1} \tag{9}$$

$$v_i^{t+1} = v_i^t + c_1 r_1^t \left[P_{best.i}^t - z_i^t \right] + c_2 r_2^t \left[G_{best.i}^t - z_i^t \right] \tag{10}$$

- $G_{best.i}^t$ and $P_{best.i}^t$ are the global and local best position
- c_1 and c_2 are the positive acceleration coefficients
- z_i^t and v_i^t are the particle position and velocity
- r_1^t and r_2^t are the random values between [0, 1]

The particle positions in the PSO are the potential solutions representing duty cycles.

3.1.3. MFO-MPPT

In the proposed MFO-MPPT control strategy, the total number of search operators is defined to be 27 with the iteration number 90. The objective function for MPPT is given in (11).

$$f(I_{PVi}, V_{PVi}) = \frac{d(P = I_{PVi} V_{PVi})}{dV_{PVi}} \tag{11}$$

where, I_{PVi}, V_{PVi} are the PV output current and voltages, respectively.

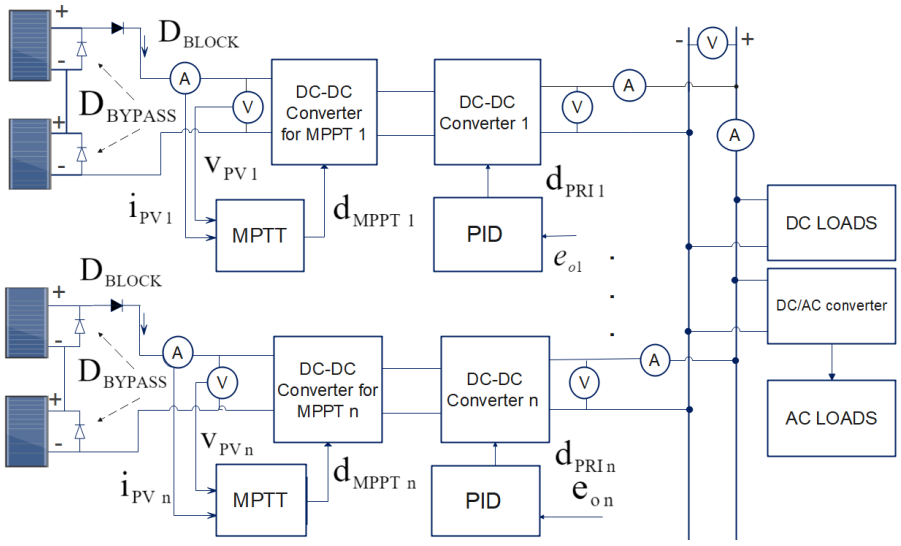

Figure 2. Simple PV-DC microgrid with MPPT [4]

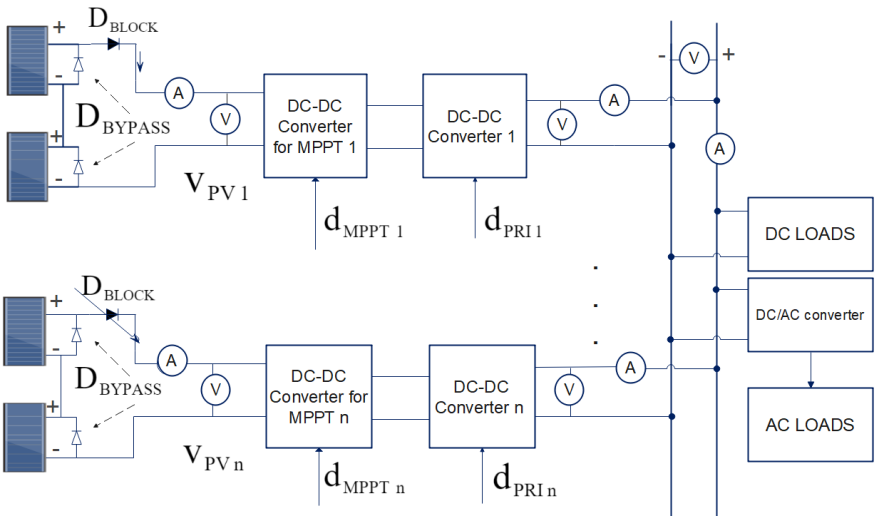

Figure 3. PV-based DCMG structure with the proposed controller

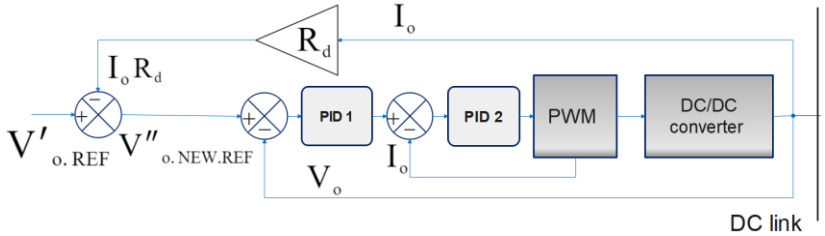

Figure 4. Traditional droop control technique [21]

3.2. Primary Controller

3.2.1. Traditional Droop Control

The primary purpose of the droop control is to equate the output currents among the parallel connected units by the addition of virtual resistance, which does not generate heat as opposed to the real resistance. The general droop-control structure is presented in Figure 4. Equation (12) presents the general mathematical model of droop control for the parallel connected converters [22].

$$V''_{O.J.NEW.REF} = V'_{O.REF} - I_{oj} R_{DROOPJ} \quad (12)$$

where, $V''_{O.J.NEW.REF}, V'_{O.REF}, I_{OJ}, R_{DROOPJ}(R_D)$ are the new reference, the reference voltage (before droop applied), output current and droop resistance of the *J*th converter, respectively. The droop gain for the permissible voltage deviation can be determined by (13).

$$R_{DROOPJ} = \frac{\left(V''_{O.J.NEW.REF} - V'_{O.REF}\right)}{I_{oj}} \quad (13)$$

3.2.2. Proposed Droop Control

MFO droop gains are proposed to solve issues concerning constant droop gains. An objective function is necessary to execute the algorithm. To formulate the objective function, two essential steps must be taken. The first step requires the standard variation minimization of output converter currents. Supposing there are *n* converters with the corresponding output currents $\left(I_{O.1}, I_{O.2}, I_{O.3} \ldots I_{O.N}\right)$. Under ideal conditions, all these output currents $\left(I_{O.1,} = I_{O.2,} = I_{O.3} \ldots = I_{O.N}\right)$ are equal to one another, but the non-ideal nature of processes and converters the output current may all be not the same, increasing stress on some of the converters. To formulate the objective function for the primary controller an inclusion of the output current standard deviation is proposed. However, as known, in droop control methods, the better the current sharing is, the larger the voltage deviation is. To reach a compromise between perfect current sharing and permissible voltage deviation, the integration of the voltage deviation to the objective function is suggested in Equation (14).

$$f_{obj}(\sigma_i, \Delta V_{errj}) = \sqrt{\frac{\sum (I_{OJ} - \bar{I})}{N}} + \sum \left| V_{MG.REF} - V_{OJ} \right| \quad (14)$$

where, $\sigma_i, I_{O.J}, \bar{I}, \Delta V_{errj}, V'_{MG.REF}, V_{O.J}$ are the standard deviation, *J*th converter actual output current, average output currents, voltage deviation error, the reference voltage, and actual output voltage, respectively.

Figure 5 describes the proposed strategy with the MFO-primary controller.

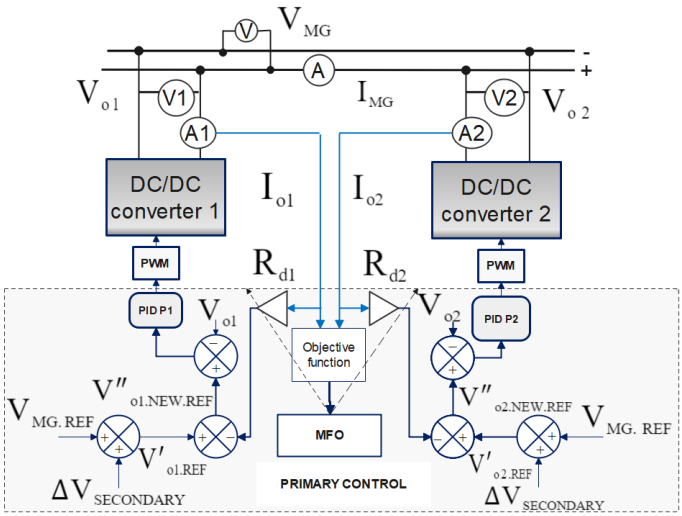

Figure 5. Proposed MFO-based primary controller

3.3. Secondary Control

The principal purpose of the secondary controllers is to reduce any possible voltage deviation on the common DC link with the help of PI/PID controllers. The actual microgrid voltage (V_{MG}), is subtracted from the reference microgrid voltage ($V_{MG.REF}$), before it is fed to the PID controller and the formulas are given in (15) and (16) [22].

$$e_{MG} = (V_{MG.REF} - V_{MG}) \quad (15)$$

$$\Delta V_{secondary} = K_p e_p + K_i \int e_p dt + K_d \frac{de_p}{dt} \quad (16)$$

where, K_p, K_i, K_d are PID proportional, integral, and derivative gains. Having formulated $\Delta V_{secondary}$, the droop gain equation can be updated as (17).

$$V''_{O.J} = V'_{MG.REF} - I_{O.J} R_{DROOPJ} + \Delta V_{secondary} \quad (17)$$

where, $V''_{O.J}$ are the new reference voltages for the *j*th converter.

3.4. Tertiary Control

Tertiary control is used to control the power flow between DC microgrid and the grid, among other DC microgrids. It establishes the reference output voltage for the DC microgrid. The actual microgrid power, P_{MG} is subtracted from the reference microgrid voltage P_{REF}, before it is fed to the PID controller [22]. Equations (18) and (19) represent the formula for the tertiary controller.

$$e_p = (P_{REF.MG} - P_{MG}) \quad (18)$$

$$V_{MG.REF} = K_p e_p + K_i \int e_p dt + K_d \frac{de_p}{dt} \quad (19)$$

The determined reference voltage is then applied to the primary and secondary controllers. Figure 6 depicts the proposed secondary and tertiary control strategy.

3.5. Proposed Central Controller based on MFO

The central controller is proposed to implement a hierarchical control strategy to improve efficiency. The proposed controller implements MPPT, primary, secondary, and tertiary control strategies with a unified MFO algorithm and is shown in Figure 7. Two fundamental objective functions are defined for the MFO algorithm. The first objective function is the Equation (11).

The output is duty cycles fed to the switching electronic elements of the first converter to extract maximum power from the input stage of the second converter. The second objective function is the Equation (14). The droop gains (virtual resistance values) are obtained as a result of objective function minimization. The primary controller also inputs corrective voltage $\Delta V_{secondary}$ from the secondary controller.

The iteration number and moth numbers are selected to be 20 and 30, respectively. The higher the number of moths and iterations, the better the result is. However, increasing the numbers may also cause an additional computational burden on the controllers.

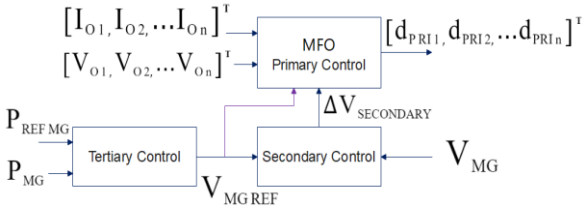

Figure 6. Proposed tertiary and secondary control

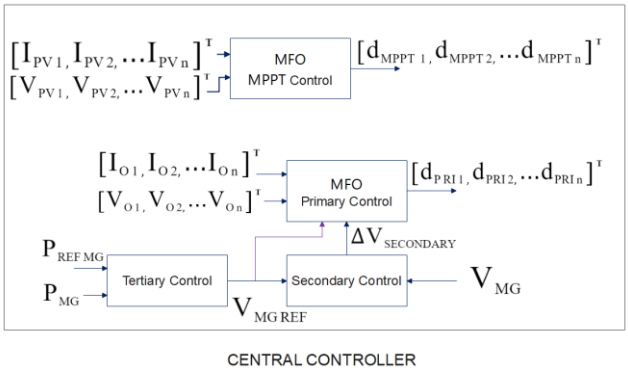

Figure 7. Proposed central controller with hierarchical strategy

4. SIMULATION RESULTS

Figure 8 depicts the presence of multiple maximum points in the power-voltage (P-V) characteristics of the PV unit under partial shading consideration. The maximum peak exists at 62 V with the highest power of 77 W, while the remainders are the local peaks. Simulations are carried out to evaluate the ability to detect the global peak. Five photovoltaic units with various irradiance levels and 25 Celsius temperatures are chosen, which are illustrated in Table 2. As is shown, the global maximum power is 83.95 W at 61.88 V. The local maxima are 39.81 W at 18.05 V, 71.92 W at 40.02 V, 76.87 W at 85.01 V, and 48.081 W at 105.012 V. Figure 9 compares the followed PV power in MFO, PO, and PSO-MPPT trackers. MFO and PSO-MPPT strategies managed to follow the desired global peak, at 83.95 W, while, the PO MPPT obtained the maxima at about 76.87 W. Although both PSO and MFO-MPPT trackers tracked the global peak, MFO had a settling time of 0.61 s, while that for PSO-MPPT was around 2.99 s. The voltage of the observed maximum power for PSO, MFO, and PO-MPPT is 61.88 V, 61.88 V, and 84.97 V, respectively. The module output current is depicted in Figure 9.

The numerical data and PV inputs are presented in Tables 2 and 3, respectively. Figure 10a, describes the standard deviation of output currents among the units in a DCMG. As is shown, the MFO-MPPT tracker managed to reduce the output current differences among units to near-zero values, whereas there is considerable variation with the conventional droop strategy under dynamic variations. Figure 10d illustrates the power-sharing between the units with the traditional droop. Voltages of the converters are varied from 24.75 to 25.25 V, as given in Table, to imitate the output voltage variation and cause artificial unequal current sharing. From time 0.1 s to 0.5 s the output voltages of both units are 25 V and the difference in power is minimal. From time 0.5 s to 0.7 s, the unit-1 and the unit-2 output voltage are 25 V and 24.75, respectively. All the outputted power is from unit 1. From time 0.8 s to 0.9 s, the unit-1 and the unit-2 output voltage are 25.25 V and 25 V, respectively. All the outputted power is from unit 2. The small variation in the output voltages is able to cause a large difference in the unit power sharing. Figure 10b illustrates the unit output voltages to assess the degree of voltage deviation as a result of droop control. Figure 10c illustrates the power-sharing between the units with the MFO droop. Compared with the traditional droop the proposed droop control minimized the difference in power. The numerical data are presented in Table 5.

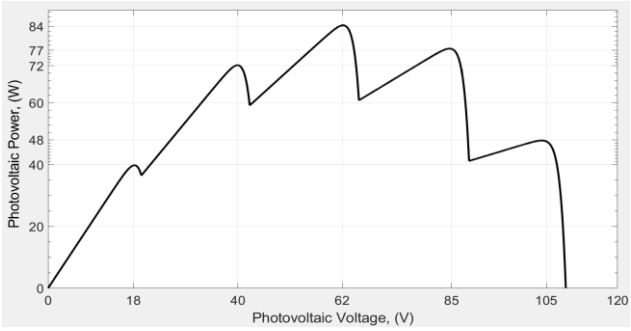

Figure 8. *P-V* characteristics of solar modules under partial shading

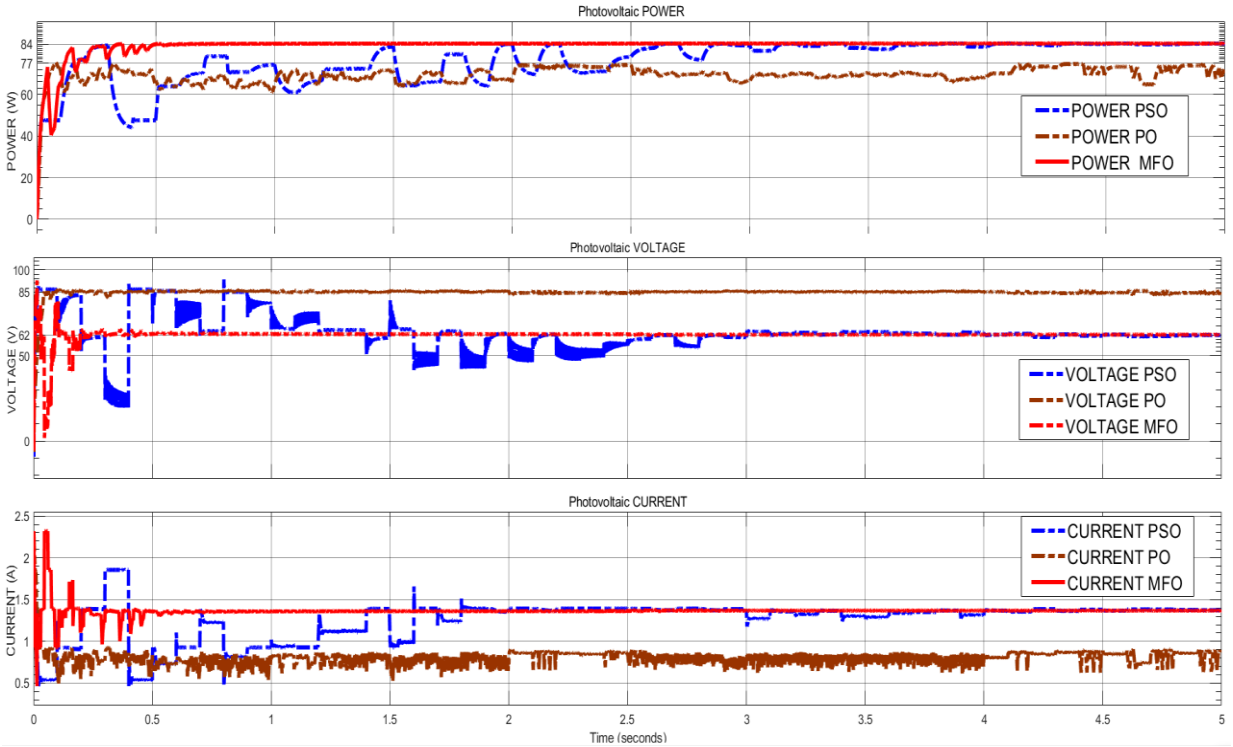

Figure 9. MPPT controller performance

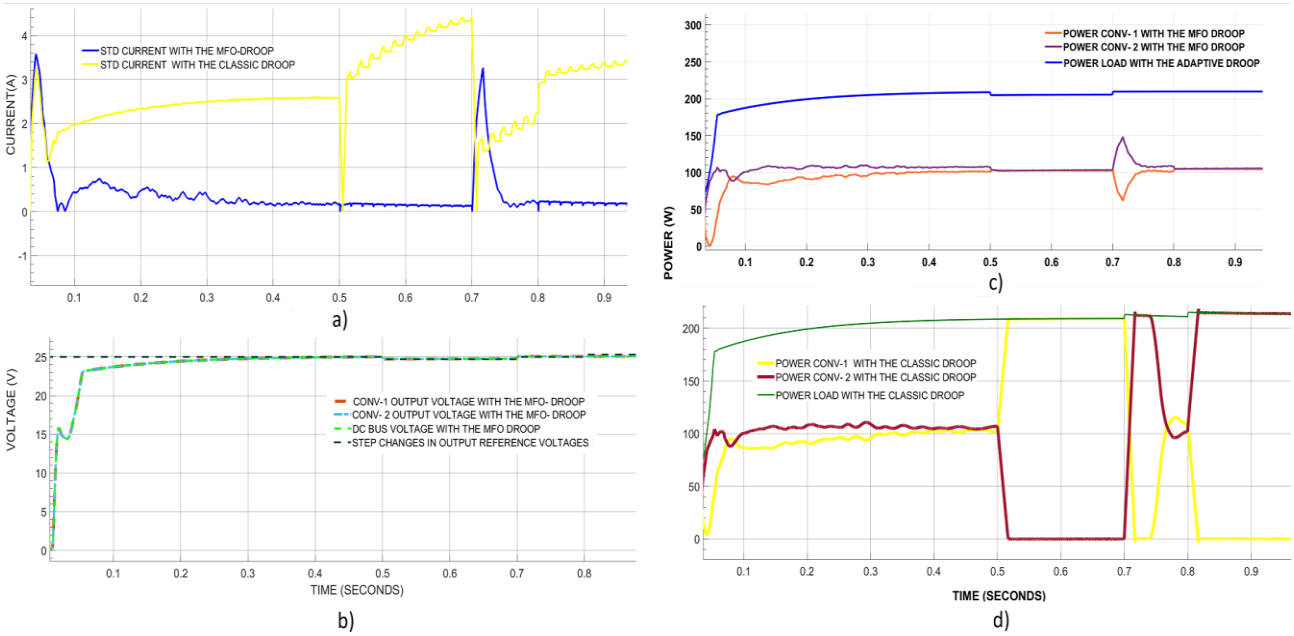

Figure 10. Proposed primary controller output response, a) STD current, b) output voltage, c) power-sharing with MFO-droop, d) power-sharing classic droop

Table 2. PV input

PV parameters	M1(module1)	M.2	M.3	M.4	M.5
Irradiation (W/m^2)	850	590	850	415	640
Temperature (Celsius)	25	25	25 V	25	25

Table 3. PV data

MPPT Controllers	PO	PSO	MFO
Tracked Maximum power	61-77 W	83.95 W	83.95 W
Voltage	84.97 V	61.88 V	61.88 V
Relative Convergence Speed	Low or zero	Moderate	Fast

Table 4. Change of Duty ratio in PO method

Time (second)	0.1-0.5 s	0.5-0.7 s	0.8 s	0.9 s
Reference Voltages	25 V	24.75 V	25 V	25.25 V

Table 5. Numerical data for classical/proposed droop

Reference Voltages	25 V	24.75 V	25.25 V
Current STD	2.35/0.4	4/0.2	3.4/0.25
Avg. Current difference (A)	3.4 /0.15	5.5/2	4.6/0.35
Avg. Power difference (W)	(15-6)/6	200/7.8	220/8
Avg. Voltage difference (V)	0.05/0.01	0.2/0.23	0.1/0.12

5. CONCLUSIONS

A hierarchical control system with a moth-flame optimized central controller is proposed. Two principal objective functions are put forward to improve power-sharing with the MFO-droop control method and MPPT controller. Partial shading conditions are considered for the MFO-MPPT to assess its efficiency. As a result, the global maximum is tracked. Considering the primary controller, droop gains are varied to adapt to the changes in output voltage/currents. Furthermore, the proposed MFO-based central controller integrates tertiary and secondary controllers.

REFERENCES

[1] R. Kandari, Neeraj, A. Mittal, "DC Microgrid", Microgrids, pp. 91-139, 2022.

[2] U. Manandhar, A. Ukil, T.K. Kiat Jonathan, "Efficiency Comparison of DC and AC Microgrid", IEEE Innovative Smart Grid Technologies - Asia (ISGT ASIA), pp. 1-6, 2015.

[3] A.O. Kucuk, H. Gozde, M.C. Taplamacioglu, M. Dursun, "Investigation of Partial Shading Effects on Photovoltaic Systems According to Different Connection Types", International Journal on Technical and Physical Problems of Engineering (IJTPE), Issue 38, Vol. 11, No. 1, pp. 31-34, March 2019.

[4] J.A. Ramos Hernanz, J.M. Lopez Guede, I. Zamora, P. Eguia, E. Zulueta, O. Barambones, "Analysis of the Algorithm P&O for MPPT", International Journal on Technical and Physical Problems of Engineering (IJTPE), Issue 31, Vol. 9, No. 2, pp. 6-14, June 2017.

[5] D. Guiza, D. Ounnas, Y. Soufi, A. Bouden, M. Maamri, "Implementation of Modified Perturb and Observe Based MPPT Algorithm for Photovoltaic System", The First International Conference on Sustainable Renewable Energy Systems and Applications (ICSRESA), pp. 1-6, 2019.

[6] V.K. Yadav, S.K. Jha, B. Kumar, "Comparative Study of Different Variable Step Size Perturb and Observe based MPPT", International Conference on Advances in Computing, Communication and Materials (ICACCM), pp. 272-277, 2020.

[7] P.K. Vineeth Kumar, K. Manjunath, "Analysis, Design, and Implementation for Control of Non-Inverted Zeta Converter Using Incremental Conductance MPPT Algorithm for SPV Applications", International Conference on Inventive Systems and Control (ICISC), pp. 1-5, 2017.

[8] E. Kim, M. Warner, I. Bhattacharya, "Adaptive Step Size Incremental Conductance Based Maximum Power Point Tracking (MPPT)", The 47th IEEE Photovoltaic Specialists Conference (PVSC), pp. 2335-2339, 2020.

[9] U. Chauhan, A. Rani, V. Singh, B. Kumar, "A Modified Incremental Conductance Maximum Power Point Technique for Standalone PV System", The 7th International Conference on Signal Processing and Integrated Networks (SPIN), pp. 61-64, 2020.
[10] D. Lakshmi, M. R. Rashmi, "A Modified Incremental Conductance Algorithm for Partially Shaded PV Array", International Conference on Technological Advancements in Power and Energy (TAP Energy), pp. 1-6, 2017.
[11] Zhanghong, Lishengzhu, Zhangxiaonan, Xiayilan, "MPPT Control Strategy for Photovoltaic Cells Based on Fuzzy Control", The 12th International Conference on Natural Computation, Fuzzy Systems and Knowledge Discovery (ICNC-FSKD), pp. 450-454, Changsha, China, 2016
[12] M.L. Shah, A. Dhaneria, P.S. Modi, H. Khambhadiya, K.K.D, "Fuzzy Logic MPPT for Grid Tie Solar Inverter", IEEE International Conference for Innovation in Technology (INOCON), pp. 1-6, 2020.
[13] R. Sankar, S. Velladurai, R. Rajarajan, J.A. Thulasi, "II. PV System Description: Maximum Power Extraction in PV System Using Fuzzy Logic and Dual MPPT Control", International Conference on Energy, Communication, Data Analytics and Soft Computing (ICECDS), pp. 3764-3769, 2017.
[14] N.M. Tabatabaei, S.R. Mortezaei, A.J. Abbasi, S. Gorji "Maximum Power Point Tracking of On-Grid Photovoltaic Systems by Providing a Fuzzy Intelligent-Pso Method Based on A Controllable Inverter with Adaptive Hysteresis Band", International Journal on Technical and Physical Problems of Engineering (IJTPE), Issue 37, Vol. 10, No. 4, pp. 15-24, December 2018.
[15] L. Xu, R. Cheng, Z. Xia, Z. Shen, "Improved Particle Swarm Optimization (PSO)-Based MPPT Method for PV String Under Partially Shading and Uniform Irradiance Condition", Asia Energy and Electrical Engineering Symposium (AEEES), pp. 771-775, 2020.
[16] S. Kamalsakthi, J. Baskaran, S.A. Elankurisil, "Optimization of Grid Connected PV System by Partial Shading MPPT Using Modified PSO Algorithm", International Conference on Computation of Power, Energy, Information and Communication (ICCPEIC), pp. 298-301, 2019.
[17] M. Merchaoui, A. Sakly, M.F. Mimouni, "Improved fast Particle Swarm Optimization-Based PV MPPT", The 9th International Renewable Energy Congress (IREC), pp. 1-7, 2018.
[18] A. Karimi, A. Pirayesh, T.S. Aghdam, M. Sedighizadeh, "Analysis of Power-Sharing Based on Small Signal Stability in a DC Microgrid", International Journal on Technical and Physical Problems of Engineering (IJTPE), Issue 15, Vol. 5, No. 2, pp. 118-122, June 2013.
[19] F. Alam, M. Ashfaq, S.S. Zaidi, A.Y. Memon, "Robust Droop Control Design for a Hybrid AC/DC Microgrid", UKACC The 11th International Conference on Control (CONTROL), pp. 1-6, 2016.
[20] Q. Liu, Z. Fu, "Bus Voltage Deviation Automatic Compensation Control Based on Droop Control", IEEE 3rd Advanced Information Technology, Electronic and Automation Control Conference (IAEAC), pp. 24-28, 2018.
[21] I.U. Nutkani, W. Peng, P.C. Loh, F. Blaabjerg, "Cost-Based Droop Scheme for DC Microgrid", IEEE Energy Conversion Congress and Exposition (ECCE), pp. 765-769, 2014.
[22] S. Dahale, A. Das, N.M. Pindoriya, S. Rajendran, "An Overview of DC-DC Converter Topologies and Controls in DC Microgrid", The 7th International Conference on Power Systems (ICPS), pp. 410-415, 2017.
[23] S. Mirjalili, "Moth-Flame Optimization Algorithm: A Novel Nature-Inspired Heuristic Paradigm", Knowledge-Based Systems, Vol. 89, pp. 228-249, November 2015.
[24] M. Shehab, L. Abualigah, H. Al Hamad, H. Alabool, M. Alshinwan, A.M. Khasawneh, "Moth-Flame Optimization Algorithm: Variants and Applications", Neural Computing and Applications, October 2019.

BIOGRAPHIES

Elvin Yusubov was born in Baku, Azerbaijan in 1993. He received the B.Sc. degree in Electronics from National Aviation Academy of Azerbaijan, Baku, Azerbaijan in 2015 and the M.Sc. degree in Computerized Information Measurement and Control from Azerbaijan State Oil and Industry University, Baku, Azerbaijan in 2019. Currently, he is a Ph.D. student at Instrumentation Engineering Department, Azerbaijan State Oil and Industry University. His research interests are in the area of power electronics, PID/fuzzy control, and microcontrollers.

Bekirova Lala Rustam received the M.Sc. and Ph.D. degrees from Azerbaijan Institute of Oil and Chemistry, Baku, Azerbaijan in 1985 and 1998, respectively. She received the Doctor of Technical Sciences in 2016. Currently, she is the Associate Professor and Head of Department of Instrumentation Engineering at Azerbaijan State Oil and Industrial University, Baku, Azerbaijan. She has more than 115 articles, patents, and monographs. She was the organizer and member of international conferences and seminars, such as co-chairman of international conference on "MIMCS-2019" and "MIMCS-2020". She is also the co-founder and member of International Scientific Association of Scientists ALIM. Her fields of research include physical and technical bases of information and measurement systems, remote measurements and aerospace research, and optical engineering.